JMEPEG (2000) 9:463-466

Anelastic Deformation Measurements in Structural Engineering Alloys

J.D. Cotton

(Submitted 30 March 2000; in revised form 12 May 2000)

Keywords anelasticity, compression tests, type 4340 steel, 15-5 PH steel, type 304 steel, Ti-6Al-4V

1. Introduction

The installation of a new transonic wind tunnel[1] included replacement of the main balance, which measures forces on the model during testing. The balance flexures have several physical and mechanical property requirements. High yield strength is necessary to provide a wide elastic response range. Thermal expansion should be low and thermal conductivity and heat capacity high. This minimizes differential heating and cooling effects within the balance structure. The high precision with which displacement can be measured *via* laser interferometry permits observation of thermal and anelastic strain events in the load data. To minimize the effects of such artifacts, the deformation behavior for the beam flexures must be well understood. While thermal expansion data are commonly available for most structural alloys, anelastic strain data are not. The tests described herein were conducted to provide an initial characterization of the anelastic deformation behavior of several structural alloys under ambient conditions.

Anelasticity is defined here as the time-dependent nonelastic deformation that is recoverable on stress removal.[2] It is usually small in magnitude, less than 0.0005 strain (500 $\mu\varepsilon$), and is not usually accounted for in structural applications. Anelastic strain can originate from stress-induced ordering of interstitial and substitutional solute atoms, grain-boundary sliding, dislocation, and thermal currents resulting from elastic anisotropy of adjacent crystals.[3] Other time-dependent nonelastic deformation processes, such as creep, are not recoverable.

2. Materials and Experimental Procedures

The materials for these tests were chosen to provide a variety of deformation responses and properties since anelastic deformation data are not commonly available for structural alloys. The materials were 4340 (a high-strength, medium carbon alloy steel), 15-5 PH (a low carbon precipitation-hardening stainless steel), 304 (a common austenitic stainless steel), Ti6Al4V (a common alpha-beta titanium alloy), and NILO 365 (a recently developed, heat-treatable low-expansion iron-nickel alloy, produced by Inco Alloys, Huntington, WV).

J.D. Cotton, The Boeing Company, Seattle, WA 98055.

Nominal compositions are given in Table 1. All materials were obtained in rod form in the annealed condition, with the exception of the 15-5 PH, which was obtained in the hardened condition. The metallurgical state was confirmed by metallography and hardness measurements prior to further testing.

Compression tests of cylindrical specimens were chosen because of their ease of interpretation, constant cross section, and minimal fixture requirements. A number of compression specimens consisting of right cylinders with length/diameter = 2 were machined. The ends were machined parallel to within 1°. Single, transducer-class, WK strain gauges (Micro-Measurements Groups, Raleigh, NC) were epoxy bonded to each specimen using Micro-Measurements M-Bond 200 epoxy. These gauges were chosen for their accuracy and good creep resistance under ambient conditions. The gauge strain limit was 1.5%. All measurements were taken well within this limit. Gauge hysteresis and creep effects were estimated at less than 5 $\mu\varepsilon$ for each specimen.

Specimen loading was accomplished with a Satec (Grove City, PA) 100,000-lb load frame. Prior to testing, the load frame compliance and drift were measured by loading the empty platens to 444,822 N (100,000 lbs) for 30 min and recording any crosshead motion. The crosshead position varied less than 0.000254 cm (0.0001 in.) (measurement resolution limit) during this period.

All time-load-displacement data were digitally collected at a rate of five points per second. A series of three loading cycles was conducted on each specimen, principally to examine for strain-hardening effects. Three specimens were tested for each alloy. The first loading cycle for the first specimen of each specimen triplet was tested to 0.2% offset yield strain. This established the compressive yield strength (CYS) of the material and was the basis for choosing subsequent loads. Thereafter, the test sequence consisted of loading the specimen to 70% of the measured 0.2% CYS in less than 1 s. The short loading time was intended to minimize any time-dependent effects. The stress was maintained in load control for 30 min, during which the specimen length was recorded, and then was removed as quickly as possible. The specimen length was recorded for another 30 min at zero applied load. This load cycle was conducted in triplicate for the second and third specimens of each alloy series.

The data were digitally collected for each test and plots of strain versus time produced. By measuring the strain accumulated at full load, and then at zero load, estimates of the anelastic component of the strain were determined and analyzed.

Table 1 Nominal alloy compositions (wt.%) and initial rod diameters (cm)

Alloy	C	Si	Mn	Cr	Mo	Ni	Fe	Other	Diam.
4340	0.35	0.25	0.7	0.8	0.25	1.85	Bal	. . .	1.588
15-5 PH	0.07	1.0	1.0	15	. . .	4.5	Bal	3.5 Cu; 0.3 Nb	1.905
304 SS	0.08	1.0	2.0	20	. . .	8	Bal	. . .	0.953
Ti6Al4V	0.1	. . .	. . .	. . .	. . .	. . .	. . .	6Al; 4V; bal Ti	1.270
NILO 365	0.02	. . .	. . .	. . .	. . .	43.5	Bal	1.4 Ti; 3.3 Nb	0.551

Table 2 Time-dependent compressive strain at 70% of 0.2% CYS (loading) and zero stress (unloading) (strain × 10^{-6})

Alloy →	4340		15-5 PH		304 SS		NILO 365		Ti6Al4V	
Load (Mpa) →	413		722		420		255		722	
Specimen no. – Cycle no.	Load	Unload	Load	Unload	Load	Unload	Load	Unload	Load	Unload
1-1	← Loaded to 0.2% plastic strain and unloaded →									
1-2	28	−23	35	−30	188	−33	15	11	(a)	(a)
1-3	22	−23	25	−18	(b)	(b)	14	18	(a)	(a)
2-1	344	−33	83	−19	(b)	(b)	−15	3	(a)	(a)
2-2	38	−23	(a)	(a)	(b)	(b)	−12	5	(a)	(a)
2-3	27	−22	(a)	(a)	(b)	(b)	−16	16	(a)	(a)
3-1	329	−25	56	−27	196	−32	30	12	18	−4
3-2	118	−24	33	−25	42	−26	38	8	(a)	(a)
3-3	35	−30	27	−25	30	−24	2	9	(a)	(a)

(a) Strain gage detached
(b) Specimen overloaded

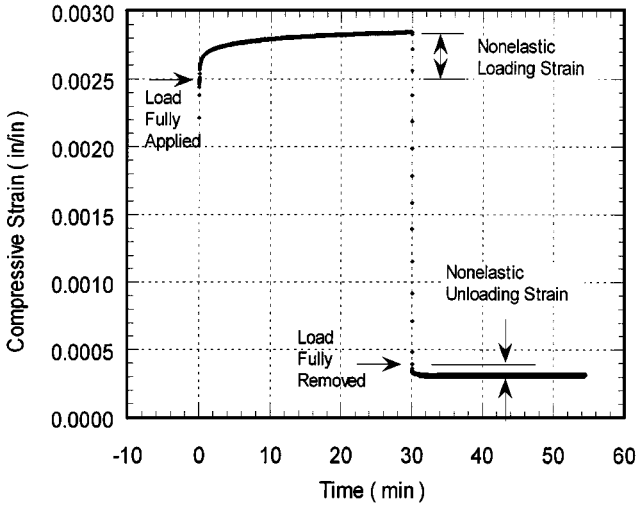

Fig. 1 Strain-time behavior for 4340 steel, test #number 2-1

3. Results

A typical strain-time plot is shown in Fig. 1. In this plot, the strain at which 0.7 CYS was reached is indicated ("Load Fully Applied"). Strains accumulated after that point in time were considered nonelastic. A distinction is made between "nonelastic" and "anelastic," in which anelastic is considered a subset of possible nonelastic processes. Nonelastic strain includes all irreversible (due to glide, climb, most phase transformations, and twinning) as well as reversible (anelastic) strain. Upon unloading, all time-dependent strain is termed anelastic after the instantaneous elastic contraction. In this particular example, the bulk of the nonelastic loading strain is not recovered on unloading.

A gross metric of time-dependent strain was taken as the total strain accumulated on loading for 30 min, and then the total strain recovered on unloading for 30 min. These values are given in Table 2 for each test.

4. Discussion

The strain behaviors depended upon alloy class. As a group, the ferrous alloys (4340, 15-5 PH, and 304 SS) were similar. Each showed irrecoverable strain during the initial loading cycle that diminished in magnitude with each loading cycle (Fig. 2). This irrecoverable strain is presumably due to primary creep. By the third cycle, the 30-min loading and unloading strains were within about 5 $\mu\varepsilon$ of one another, and the cumulative anelastic strain for these alloys was consistently about 25- to 30 $\mu\varepsilon$ for this time frame. Although the 15-5 PH was considerably stronger than the 4340 and 304 SS, its anelastic behavior was comparable (Fig. 2 and 3).

Strain in the Ti6Al4V alloy was small and unremarkable, although this is based on a single measurement. Considerable difficulty was encountered in maintaining a sound bond between the strain gage and the specimens. This was partly due to the

nature of the titanium surface film and partly to the high yield strength-to-modulus ratio and subsequent large strains for the rod obtained for this study. Based on this single test, the recovered anelastic strain for Ti6Al4V was only 4 $\mu\varepsilon$. However, this was not greatly different from the constant-stress loading strain.

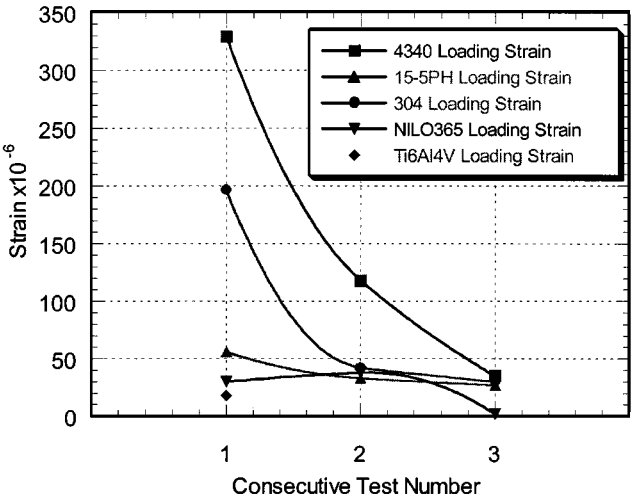

Fig. 2 Nonelastic loading strain vs consecutive load cycle (third specimens)

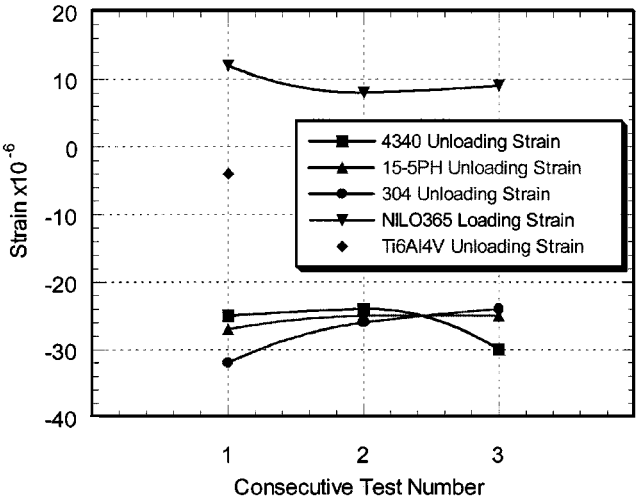

Fig. 3 Nonelastic (anelastic) unloading strain vs consecutive load cycle (third specimens)

Unusual behavior was sometimes exhibited by the NILO 365, *i.e.*, a negative recovery strain (it expanded upon load release). Furthermore, as shown in Table 2, specimen 2 increased in length during compression. This anomalous strain behavior may be due to the known lattice instabilities that occur in Invar-type alloys. These are related to the effects of pressure on magnetostriction and impending martensitic phase transformations.[4,5,6] Despite this response, the mean anelastic/magnetostrictive strain on unloading was 10 $\mu\varepsilon$, less than the ferrous alloys.

Although not the focus of this work, the question remains as to what anelasticity *mechanism* is dominant in the materials of the present study. Quantitative methods for determining mechanisms have not been developed, although anelasticity in ferrous alloys has been ascribed to interstitial diffusion to dilated lattice sites.[7] However, attempts to fit the strain recovery curves to a logarithmic decay function were not satisfactory, which suggests that interstitial diffusion is not responsible.

Most recent research points to thermally activated glide due to the advance or unbowing of pinned dislocations as the predominant mechanism.[8,9,10] During loading, dislocation segments react to applied stress by bowing to a metastable position. Additional glide is time dependent, arising from the statistics of climb, cross-slip, or reaction to an easy slip plane. This results in primary creep (or secondary creep transients on a load change) and was especially apparent in the initial loading cycles of the 4340 and 304 SS alloys. On unloading, back stresses on the pinned segments between "hard" regions of the substructure produce the opposite effect—again thermally activated–resulting in a recovery of a portion of the loading strain.

Since thermal activation is essentially a diffusional process, one would expect the degree of room-temperature anelasticity to scale inversely with absolute melting point. This would explain the similarity of the behavior of the ferrous alloys. The predominant crystal structure of the alloy does not appear to be critical in this regard, since ferritic, austenitic, and hexagonal alloys were represented in the present study and were not significantly different in their behavior.

It might be argued that measurements at such small strains are subject to artifacts such as gage creep, adhesive creep, thermoelastic heating, and temperature fluctuations. While these are valid potential sources of error, the regular data trends, and differences between alloy classes, lend credence to the present results. Estimates of thermoelastic heating due to isoentropic compression were calculated[1] by the expression

$$\delta T/\delta\varepsilon\big|_s = -V_m\alpha ET/C_v$$

Table 3 Thermoelastic heating estimation

Alloy	V_m (cm^3/mole)	α (1/K)	E (Pa)	T (K)	C_v (J/g - K)	$dT/d\varepsilon$ (K/strain)	ΔT (K)
4340	0.1397	1.15E-05	1.93E + 11	298	0.487	−3.40	0.0073
15-5 PH	0.1397	1.08E-05	2.00E + 11	298	0.462	−3.48	0.0126
304 SS	0.1415	1.73E-05	1.93E + 11	298	0.504	−5.00	0.0109
NILO 365	0.1439	4.14E-06	1.59E + 11	298	0.420	−1.21	0.0019
Ti6Al4V	0.0925	2.88E-05	1.14E + 11	298	0.567	−3.33	0.0212

The results for each material at the loading conditions of interest are given in Table 3. They show that a temperature rise of less than 0.03 K would occur in all cases. The resulting effect on modulus would be negligible, and any resulting thermal expansion would be less than 1 $\mu\varepsilon$. Hence, thermoelasticity cannot account for the present observations.

5. Summary

Nonelastic strains in the form of room-temperature primary creep and anelasticity occur at 70% of the yield strength for 4340 steel, 15-5 PH, 304 stainless steel, Ti6Al4V, and NILO 365. The amount of creep (the irrecoverable strain) diminishes with loading cycle due to work hardening. The anelastic strains are relatively constant for each loading cycle, about 25 $\mu\varepsilon$ for the ferrous alloys and 4 $\mu\varepsilon$ for the Ti6Al4V. The anelastic behavior for the NILO 365 was anomalous, presumably due to magnetostriction effects.

References

1. *The Boeing News*, The Boeing Company, Seattle, WA, Sept. 17, 1996.
2. A.S. Nowick and B.S. Berry: *Anelastic Relaxation in Crystalline Solids*, Academic Press, New York, NY, 1972, p. 1.
3. G.E. Dieter: *Mechanical Metallurgy*, McGraw-Hill, New York, NY, 1976, p. 434.
4. J.W. Carr: *J. Magn. Mater.*, 1979, vol. 10, p. 197.
5. S. Steinemann, E. Toeroek, and E.Z. Wohlfarth: *Solid State Commun.*, 1976, vol. 18(5), p. 581.
6. T. Kakeshita, K. Shimizu, R. Tanaka, S. Nakamichi, S. Endo, and F. Ono: *Mater. Trans. JIM*, 1991, vol. 32 (12), p. 1115.
7. R.E. Reed-Hill: *Physical Metallurgy Principles*, D. Van Nostrand, New York, NY, 1973, p. 433.
8. G.J. Lloyd, and R.J. McElroy: *Acta Metall.*, 1974, vol. 22, p. 339.
9. J.C. Gibeling, and W.D. Nix: *Acta Metall.*, 1981, vol. 29, p. 1769.
10. J.C. Gibeling: *Acta Metall.*, 1989, vol. 37 (12), p. 3183.